

## The Role of Interactions in Systems of Single Domain Ferrimagnetic Iron Oxide Nanoparticles

Silvio Dutz\*, Rudolf Hergt

*Institute of Photonic Technology, Department Nano Biophotonics, Albert-Einstein-Straße, 9, 07745 Jena, Germany*

(Received 09 March 2012; published online 07 May 2012)

Magnetic nanoparticles are interesting materials for a lot of medical and technical applications. A less experimentally investigated question is the influence of particle packing density on magnetic properties due to magnetic interactions between single particles. For this, magnetic nanoparticles of iron oxides prepared as fine dry powder by laser deposition are investigated with respect to their structural and magnetic properties as function of packing density. The particles are nearly spherically shaped single crystals in the magnetic single domain size range with a mean diameter of 21 nm occasionally exhibiting spinel growth facets. Powders of these particles are diluted by nonmagnetic silicon oxide particles in a range of volume concentrations from 0.2 % up to 68 % of the bulk density of magnetite. The concentration dependence of remanence, coercivity and hysteresis losses is determined by measurements of minor loops in a vibrating sample magnetometer. Results which are discussed in the frame of present theoretical models may be understood in terms of the cubic anisotropy of magnetite distorted by a small uniaxial shape contribution.

**Keywords:** Magnetic interactions, Packing density, Coercivity, Magnetic nanoparticles, Magnetite.

PACS numbers: 75.50.Tt, 75.75.+a

### 1. INTRODUCTION

Magnetic nanoparticles found in last time increasing interest in a variety of applications in biology, medicine and technique [1, 2]. For decades, magnetic iron oxide particles attracted much interest in recording industry [3]. Moreover, already since long time much work in particle magnetism was performed in geology with respect to rock magnetism [4]. In medicine and technique several applications of magnetic particle dispersions for heating processes were suggested. Besides the medical applications like hyperthermia [5, 6], there are also technical ones e.g. for bonding of non-conducting media [7]. For all of these applications the viscosity of the suspension medium may vary from aqueous-like up to high values being typical for applications in technique (e.g. polymers) or medicine (cytoskeleton). In comparison, completely immobilised particles in solid dispersions are of interest, e.g. in recording or paläomagnetism. In any case, the volume concentration of the nanoparticles, their dispersion and agglomeration may influence seriously the magnetic properties of the particle system and currently are of eminent technological importance.

Besides single particle properties like saturation magnetic particle moment or crystal anisotropy, the averaged magnetic properties of the particle ensemble, in particular remanence and coercivity determine their useful properties, e.g. the heating power of particles excited by an external high frequency magnetic field. For the averaged magnetic properties of the magnetic system – in addition to the single particle magnetic properties – also the particle size distribution and possible interactions between particles are important. Both effects – size distribution and particle interactions – may influence the amount of specific loss power generated in a magnetic particle system. For optimisation of the latter one it is desirable to understand both effects separately. While the effect of particle size distribution

on the specific loss power was analysed recently within the frame of a semi-empirical model of hysteresis losses [8] there is a lack of understanding the role of interaction, yet. Evidence for the influence of particle agglomeration effects on the specific hysteresis loss power in systems of very small particles was demonstrated clearly by Eggeman et al. [9].

Magnetic particle interactions are of interest from a more fundamental point of view, too. In literature mainly theoretical work on the concentration dependence of magnetic properties of particle systems may be found [10]. In comparison, there are rare experimental investigations on real particle systems, mainly for the case of highly anisotropic particles like acicular or Co-doped iron oxide for recording applications [11, 12]. In general, particle interactions depend not only on the mean distance between particles, i.e. the concentration of the dispersion, but also seriously on the particular distribution of inter-particle distances including clustering or agglomeration effects.

It is the goal of the present paper to elucidate experimentally the role of interaction effects in magnetic particle dispersions. For this aim, the dependence of hysteresis loops on packing density of the particles is investigated. For laser evaporation prepared powders the effect of the packing density is controlled by defined mixing of the iron oxide particles with nonmagnetic silicon oxide. After structural characterisation of the particle systems their magnetic properties coercivity, relative remanence, and losses determined from integration of hysteresis loops are investigated in dependence on the volume concentration of the particle system.

### 2. BASICS

Already three decades ago it was shown by Chantrell [13] by means of two-dimensional Monte-Carlo simulations that dipolar chains and flux closure configurations might form in a magnetic particle system.

\* [silvio.dutz@ipht-jena.de](mailto:silvio.dutz@ipht-jena.de), tel.: 0049 3641 206317, fax: 0049 3641 206139

Later on, Chantrell [14] compared theoretical and experimental results in his survey on interaction effects in fine particle systems. More recently, the formation of dimers, trimers and larger aggregates due to dipolar interaction in stable ferrofluids was computed by means of Monte Carlo simulation by Castro et al. [15]. The authors point out that the results are in fair accordance with experimental observations carried out by means of birefringence of other authors. Below about 1 % volume fraction the relatively small part of agglomerated particles are only dimers. Above about 10 % volume fraction more than half of the particles are bound in agglomerations larger than trimers. The occurrence of chains in magnetite dispersions having a mean particle diameter of 21 nm was proved by Klokkenburg et al. [16] by means of cryo-TEM. In comparison, these authors did not observe chain formation in a 16-nm dispersion. Of course, the tendency for agglomeration increases seriously with the transition from superparamagnetic to stable ferromagnetic single domain. The chain formation for relatively large particles (about 30 nm diameter) is well known from magnetotactic bacteria synthesizing fine magnetite crystals [17]. In wet-chemically precipitated iron oxide suspensions clusters of about 50 nm diameter may be covered by a common shell of carboxymethyl dextran [18] forming so-called multicore particles. Larger loose aggregations often observed in transmission electron microscopy (TEM) may be due to preparation artefacts of the TEM specimens as shown by Klokkenburg et al. [16].

A comprehensive evaluation of different numerical methods for simulation of the quasistatic remagnetisation processes in fine magnetic particle systems was given by Berkov [10] for a system of identical uniaxial particles. There, the transition from single particle to collective behaviour with increasing volume concentration is discussed in dependence on the particle magnetic anisotropy. As presently best suited, the calculations of Berkov will be used below for comparison with the present experimental results though obviously there are deviations between experiment and the suppositions of that theory.

Experimentally, particle interactions may be detected by measuring different types of hysteresis minor loops, results of which may be evaluated by means of so-called Henkel plots [19]. Another empirical evaluation method is the Day plot applied currently in the field of rock magnetism [4] though the latter has some drawbacks and consequently will not be considered here.

Of course, magnetisation loops of solidified particle systems differ essentially from those of particles in liquid suspension. It has to be pointed out that – apart of ferrofluids – most practical interest in magnetic particles refers to nearly immobilised particles [20]. Accordingly the majority of experimental work done beyond the superparamagnetic size range (i.e. around 18 nm for magnetite) was performed at immobilised particles. There, particles are either in form of powders or are dispersed in a non-magnetic solid matrix (e.g. in geology or metallurgy).

### 3. RESULTS AND DISCUSSION

Figure 1a shows the saturation hysteresis loops for laser prepared particle powders of different packing

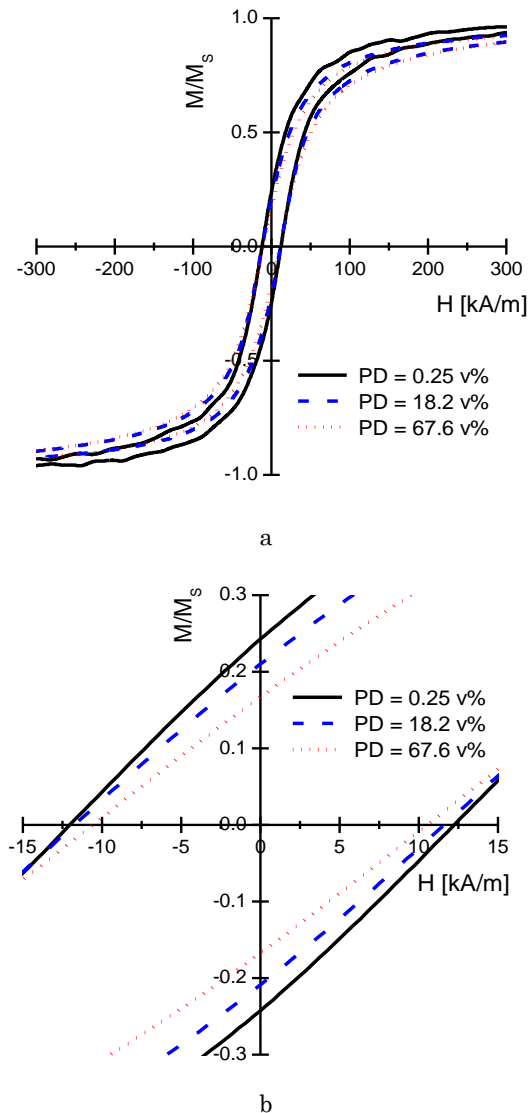


**Fig. 1** – Hysteresis loops for different packing densities (a), and zoom of the low field range for determination of the relative remanence and coercivity (b). The given magnetisation curves are normalised to the saturation magnetisation  $M_s$ .

densities. Figure 1b shows a zoom of the low field range which was used for determination of remanence and coercivity, the results of which will be discussed below. The pure particles show a saturation magnetisation ( $M_s$ ) of  $57.1 \text{ Am}^2/\text{kg}$ , a coercivity ( $H_c$ ) of  $11.8 \text{ kA/m}$ , and a relative remanence  $M_r/M_s$  of  $0.21$ .

The shape of hysteresis loops measured for samples of the concentration series shown in Figure 1a deviates considerably from loops expected in the frame of the model developed by Stoner and Wohlfarth [21] for uniaxial non-interacting single domain particles. This deviation of experiments from the SW-model is in accordance with numerous results found previously by experimental investigations of different types of single domain iron oxide nanoparticles [18, 22].

Berkov has extended the model of Stoner and Wohlfarth taking into account the effect of particle interactions by analysing the quasistatic remagnetization processes in single domain particle systems of uniaxial

anisotropy by means of numerical simulations [10]. Those results depend essentially on the parameter  $\beta = 2K/\mu_0 M_s^2$  (where is  $K$  anisotropy energy density), which measures the relative importance of anisotropy and demagnetisation energy. For large values of anisotropy ( $\beta > 5$ ) only small deviations from SW-model occur due to dipolar interactions. The effect of interactions increases with decreasing anisotropy and accordingly the shape of loops deviates increasingly from the SW result. For small values  $\beta > 0.3$  theoretical loops are mainly determined by the interaction and their shape does not much differ from loops for isotropic particles. The present authors are not aware of analogous simulations in literature for particles with cubic anisotropy.

Data determined from low field amplitude ( $H = 11$  kA/m) and saturation ( $H = 1275$  kA/m) are shown in Figures 2 and 3 in dependence on the particle volume packing density for the samples given in Table 1. The measured values of relative remanence and coercivity agree with data reported previously for single domain iron oxide powders presented by Dutz et al. [18, 22]. The experimentally found relative remanence data in Figure 2b show a moderate decrease from 0.25 for the most diluted sample to 0.17 for the most compact one and coercivity in Figure 3b from 12.1 kA/m to 10.7 kA/m, respectively. These findings follow – at least for concentrations below about 10 vol.% – the general trend of the theoretical predictions. The low relative remanence of the diluted samples may be understood

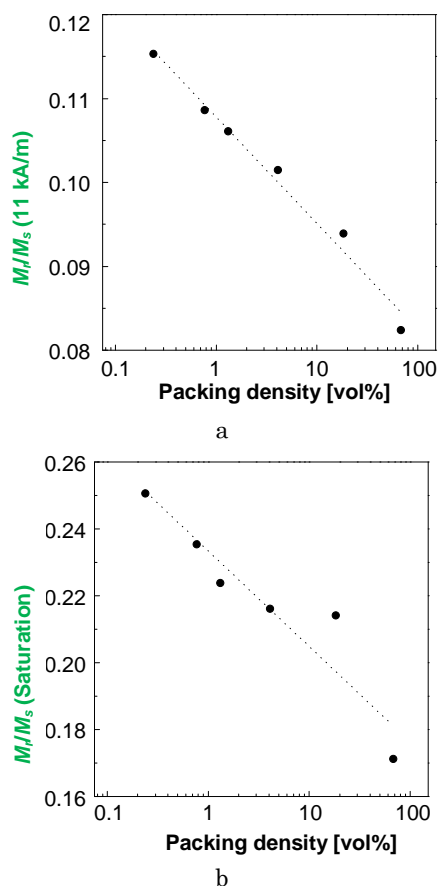


**Fig. 2** – Dependence of the relative remanence ( $M_r/M_s$ ) on packing density of magnetic nanoparticles (dots) measured at (a) low field amplitude (11 kA/m) and (b) saturation (1275 kA/m)

**Table 1** – Packing density of the prepared samples

packing density		sample density
volume%	mass%	kg/m <sup>3</sup>
0.24	3.8	12
0.77	12.3	38
1.32	21.3	66
4.08	56.8	204
18.2	100	910
67.6	100	3380

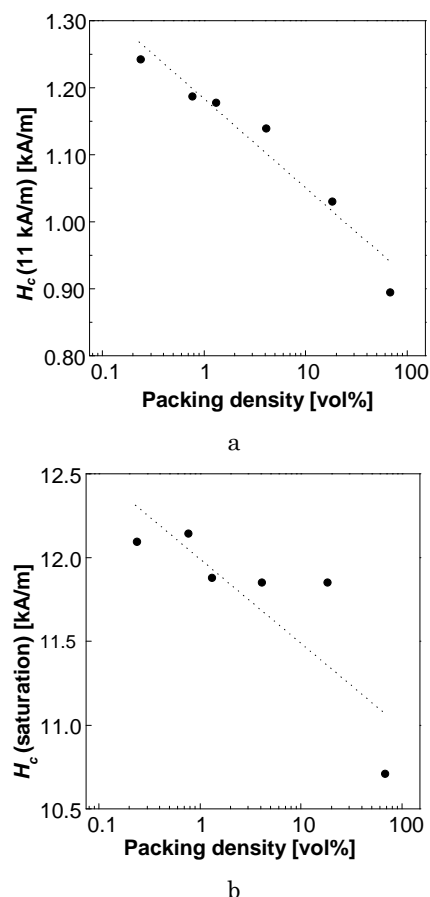


**Fig. 3** – Dependence of coercivity ( $H_c$ ) on packing density of magnetic nanoparticles (dots) measured at (a) low field amplitude (11 kA/m) and (b) saturation (1275 kA/m)

by a very low anisotropy energy density corresponding to a value of  $\beta$  below 0.1. Considering the saturation magnetisation of magnetite of 480 kA/m, values of  $\beta < 0.1$  lead to  $K < 10$  kJ/m<sup>3</sup> in accordance with expectations for the anisotropy contributions in the present particles. The crystal anisotropy of magnetite is 11 kJ/m<sup>3</sup> while maghemite has an even lower value of 4.6 kJ/m<sup>3</sup> [3]. Moreover, considering the nearly spherical shape of the particles only a small contribution due to shape anisotropy may be expected. An aspect ratio of 1.1 of a weakly ellipsoidal particle shape results in an anisotropy contribution of 3.5 kJ/m<sup>3</sup>. In general, the "effective" anisotropy energy surface of a weakly ellipsoidally stretched homogeneously magnetized particle with cubic anisotropy depends on the orientation of the shape axis with respect to the crystal lattice. In the present

case, only a small deformation with respect to the cubic anisotropy energy face is expected. The superposition of the cubic crystal anisotropy and the weak shape anisotropy may be assumed to be about  $15 \text{ kJ/m}^3$  at most. This is the case when the shape axis is parallel to the easy  $\langle 111 \rangle$  axis. For other orientations of the shape axis with respect to the crystal lattice the “effective” anisotropy is smaller. However, any such small perturbations lead to a breakdown of cubic symmetry. Accordingly, while for perfect cubic symmetry high relative remanence of 0.83 for  $K > 0$  (easy axis  $\langle 100 \rangle$ ) or 0.87 for  $K < 0$  (easy axis  $\langle 111 \rangle$ ) was predicted by theory [23], the presently observed remanence data are essentially lower. A strong decrease of  $M_r/M_s$  with increasing particle size is concluded from micromagnetic calculations for octahedral magnetite particles by Witt et al. [24]. There, the relative remanence observed in the present experiments is predicted for octahedra well above 100 nm. This again indicates that for the present particles small deviations from the ideal cubic symmetry should be taken into consideration.

However, for increasing concentration, theory predicts in the present case of low anisotropy a maximum of coercivity in dependence of packing density which is explained by Berkov as follows: Coercivity first increases with increasing concentration when dipolar interaction gains importance, but for more dense packing coercivity decreases again due to the formation of a short range order. However, this maximum of coercivity predicted by theory for intermediate packing cannot be confirmed by the present experiments. Probably, in the densely packed samples particles come locally in closer contact with each other so that a coupling due to exchange interactions may become effective and complicate magnetisation structures arise which is not considered in Berkovs model.

For minor loops measured with a low field amplitude of 11 kA/m the decrease of coercivity  $H_c$  as well as relative remanence  $M_r/M_s$  with increasing packing density shown in Figures 2a and 3a is more pronounced than for the saturation loop data discussed above.

As a common tool for checking interaction effects in magnetic particle systems the measurement of Henkel plots has proved in literature [19]. Figure 4 shows three examples of samples of different packing density prepared from laser precipitated particles. Clear deviations from the straight line holding for non-interacting particles are observed. The deviation increases with increasing packing density. Similar observations were made for wet-chemically prepared particles [22]. There, coated particles reasonably showed lower interaction than uncoated ones [18]. Nevertheless, particle systems being free of interactions in the sense of the Henkel plot were not observed experimentally till now for artificially grown iron oxide particles in the single domain size range. Reasonably, one may assume that all those samples had at least locally an essential portion of non-isolated particles.

It is known that the specific magnetic hysteresis losses (SHL) in nanoparticle powders are mainly determined by the coercivity and the relative remanence of these particles [25]. Due to this fact an increase of the mass weighted specific hysteresis losses for decreasing packing density could be expected. This was

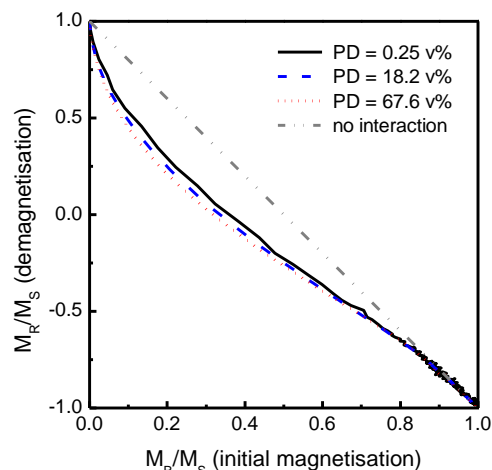


Fig. 4 – Henkel-Plots for powders of different packing density (PD) prepared by laser method

confirmed by experimental investigations with different field amplitudes. As shown in Figure 5 an increase of the specific hysteresis losses could be reached by decreasing the packing density of the powders. Remarkably, the relative increase is much more pronounced for loops measured with smaller field amplitude of 11 kA/m. Just this is of considerable practical interest since in heating processes small amplitudes are preferred due to

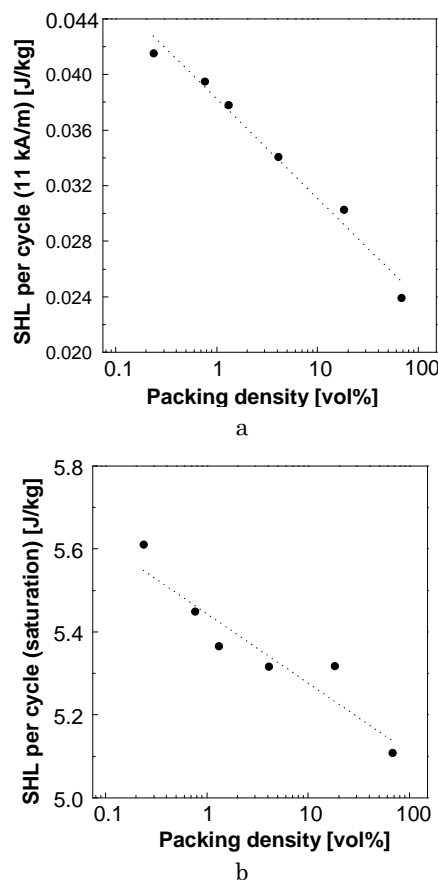


Fig. 5 – Dependence of the mass weighted specific hysteresis losses (SHL) on the packing density of magnetic nanoparticles measured at (a) low field amplitude (11 kA/m) and (b) saturation (1275 kA/m)

economical and technical reasons. In particular, for biomedical applications of high frequency heating of magnetic nanoparticles (e.g. tumor hyperthermia) field amplitude should be low enough to avoid eddy current heating of healthy tissue [1].

The dependence of specific hysteresis losses on field amplitude of wet-chemically prepared fractions gained by sedimentation was reported previously [26]. Qualitatively similar dependencies are observed in recently published results of powders of pure [22] and CMD covered particles [18]. Roughly the same dependence of specific hysteresis loss on field amplitude (Figure 5a and 5b) may be observed for laser prepared particle powders of different packing density, too. Accordingly, approximately spherically shaped magnetite particles in the single domain size range have similar magnetic properties irrespective of the way of preparation either by wet-chemical precipitation or by gas phase formation. In contrast, a remarkable difference exists between all artificially prepared iron oxide particle types on the one hand, and magnetite particles being synthesized naturally by magnetotactic bacteria which shown much smaller coercivity with higher remanence, on the other hand [27]. The perfect lattice structure of the latter ones may be the reason for these differences.

## 4. EXPERIMENTAL METHODS

### 4.1 Sample preparation

Magnetic iron oxide particles were prepared by gas phase reaction in a laser beam which results in a fine magnetite powder. For this a laser evaporation method was applied details of which were published elsewhere [28]. Starting material is a coarse hematite powder ( $\mu\text{m}$  size) which is evaporated by means of a  $\text{CO}_2$  laser. Due to the relatively steep temperature gradient outside of the evaporation zone a very fast condensation of fine particles takes place from the gas phase. The condensed particles are removed from the evaporation/condensation zone by airflow and are deposited at a filter made of paper. The resulting product is a fine powder of magnetite with a low tendency to form agglomerates. The mean particle size may be adjusted in the range from 20 to 50 nm with a relative narrow size distribution. This diameter range is just the existence range of single domain behaviour of magnetite.

For the investigation of the role of interactions for the magnetic properties, magnetic powders were diluted with appropriate volume fractions of a dry non magnetic substance (matrix) preparing in this way samples of different packing density. To obtain a preferably homogeneous mixing of magnetic and nonmagnetic particles a low agglomeration tendency of both partners is necessary. This is fulfilled in particular for the particles from laser evaporation. As a matrix material hydrophilic  $\text{SiO}_2$  powder (Aerosil® 130, Degussa, Düsseldorf, Germany) with a specific surface area of  $130 \text{ m}^2/\text{g}$  and a primary particle diameter of 16 nm was used. By adding ethanol separately to the iron oxide powder and to the matrix powder homogeneous slurries of both materials were prepared. After this, both slurries were mixed in different proportions to obtain different magnetic particle concentrations in the samples. The mixed

slurries were stirred by hand until they showed a homogeneous colour. Then the mix was ground for about half an hour in an agate mortar until they dried to a fine homogeneous powder.

The as-prepared pure laser powders had a typical density of about  $900 \text{ kg/m}^3$  measured by weighting powder of defined volume. Assuming a density of the massive magnetic material to be  $5000 \text{ kg/m}^3$  this value corresponds to a volume fraction of 18 %. An increase of the packing density of the as-prepared powder was achieved by compression of the sample at a pressure of about 350 MPa in a uniaxial press. In this way nearly 68 % of the bulk density of magnetite resulted. Table 1 shows the packing densities of samples prepared as mentioned above. The mass weighted concentrations of the samples were calculated from the sample mass and the mass of magnetic particles derived from the saturation magnetisation of the different samples by using the saturation magnetisation value of the pure particles. These values were converted into volume weighted concentrations by means of the calculated magnetic volume (from the mass and density of the particles) and the total sample volume.

### 4.2 Structural characterisation

The morphology of dry powders containing MNP may be imaged by scanning electron microscopy (SEM) and the shape, size, and agglomeration behaviour in transmission electron microscopy (TEM). A typical example of particles from powders produced by laser evaporation is shown in the TEM image of Figure 6.

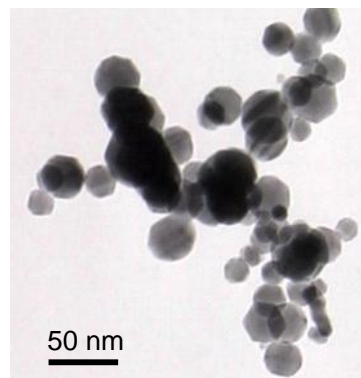


**Fig. 6** – Typical TEM image of magnetic nanoparticles prepared by laser precipitation

These particles are approximately spherical which excludes a considerable shape contribution to the magnetic anisotropy. A regular faceting due to growth planes of the spinel lattice may be recognized which indicates the perfect crystal lattice of these particles. The particles show a relatively narrow size distribution. Preparation of really monosized ferrimagnetic particles larger than 20 nm is very challenging and no satisfying results are reported in literature up to now.

The morphological observations by electron-optical imaging were supplemented by X-ray diffraction (XRD). In contrast to direct imaging, XRD yields the mean diameter of coherently scattering crystal regions. Comparing it with data from morphological determination of particle diameters one may conclude whether

the observed particles are single crystals or are composed of grains with differently oriented crystal lattice. The line width of the (440) diffraction peak gives a mean diameter of single crystal grains (evaluated by means of the Scherrer formula). For the laser evaporated particles (Figure 7) a mean diameter of 21 nm results from XRD in accordance with the results of TEM imaging. Besides information on grain size XRD allows identification of the iron oxide phase of the prepared particles. Due to the similarity of the crystal structure of magnetite and maghemite (spinel structure in both cases) very similar diffraction patterns result and a differentiation of both crystallographic phases is difficult. Therefore, and considering that the magnetic moment is not very different some authors think only of magnetite though in most cases of nanoparticles at least a mixture of both phases is present. Magnetite and maghemite may be best differentiated by scanning the (440) diffraction line with high angular resolution.

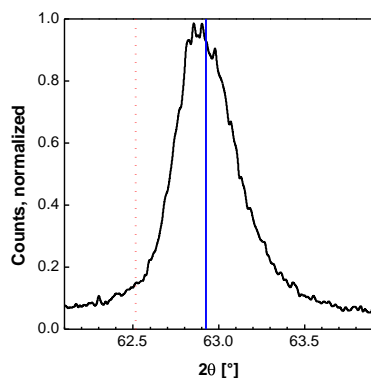


**Fig. 7** – X-ray diffraction (440) peak (Cu-K $\alpha$  radiation) of laser particles (grain size 21 nm)

In Figure 7 the measured diffraction (440) peak of laser prepared particles (grain size 21 nm) is shown. The peaks of pure magnetite (red dotted line) and maghemite (blue line) are located at  $2\theta = 62.5^\circ$  and  $2\theta = 62.9^\circ$ , respectively. The laser particles are either biphasic containing both iron oxide phases or consist of a solid solution of both phases. One may assume that their grains consist of a magnetite core covered by a surface layer which is oxidized to maghemite. The latter one is the stable phase in atmospheric conditions. Magnetite nanoparticles transform slowly into maghemite when held under contact with air – even if dispersed in an aqueous suspension which is stored in contact with air. By the way, this instability of magnetite particles is one of the reasons that magnetite is not applied by the recording industry. However, the transformation to maghemite is rather sluggish since it is hindered by relatively high diffusion barriers for oxygen in the spinel lattice. Accordingly it is observed the easier, the smaller the particles are [29].

For the dilution series of mixed powders of magnetic and nonmagnetic particles the mixing homogeneity was checked in SEM by comparing high resolution secondary electron images (SEI) with so-called composition contrast of reflected electrons. Unfortunately, some relief contrast complicates interpretation though smooth sample surfaces were tried to prepare by pressing the powder tablets against a mirror smooth surface.

The Si-oxide particles having a nominal mean diameter of about 16 nm. They may not be differentiated by morphology in the SEI. In composition contrast, iron oxide may be identified due to the much more intense scattering of the heavier iron atoms. In this way it was found that there is no remarkable clustering of iron oxide particles beyond the size observed in TEM images of the starting powder.

### 4.3 Magnetic measurements

For characterisation of the magnetic properties of the prepared nanoparticle systems hysteresis curves were measured by vibrating sample magnetometry (VSM) at saturation field amplitude (1275 kA/m) as well as at a lower field amplitude (11 kA/m). Hysteresis losses of the samples were determined by measurement of minor loops at different field amplitudes and integrating the area of these loops.

Furthermore the influence of the packing density on the interactions between magnetic particles was investigated by measuring the remanence behaviour (Henkel plot) as a function of packing density [19]. To this end the initial remanence ( $M_r$ ) for increasing field amplitudes after AC-demagnetisation was measured and plotted against the demagnetisation remanence ( $M_d$ ) for decreasing field amplitudes after magnetic saturation of the sample. Both remanence values were normalised to the value of saturation remanence.

## 5. CONCLUSIONS

The laser produced magnetic nanoparticles consist of nearly spherical single domain particles occasionally exhibiting spinel growth facets with low tendency to form agglomerates. Powders of these particles were diluted by nonmagnetic silicon oxide particles in a range of volume concentrations from 0.2 % up to 68 % of the bulk density of magnetite. By investigation of the magnetic behaviour of the particles depending on different packing densities the effect of magnetic interactions on the magnetic properties of the particle system was elucidated. Main finding is the fact that with decreasing packing density (which means a decrease of the magnetic interactions) the values for the magnetic parameters coercivity, relative remanence, and specific hysteresis losses increase. The found concentration dependence of these parameters may be understood in terms of magnetic interactions between neighbouring particles. In particular, similar magnetic interaction effects arise from low packing density up to high values of 68 % of the bulk density as proved by Henkel pots. In conclusion, the hysteresis of artificially grown nanoparticles of magnetite or maghemite in the single domain size range may be understood in terms of their cubic anisotropy distorted by a small contribution of uniaxial shape deformation irrespective of routes of their precipitation. This is in contrast to magnetite particles grown naturally by magnetotactic bacteria, which show much smaller coercivity with higher remanence.

While the diluted samples fit the theoretical model of Berkov, the dense powder samples, in particular the sample compacted by pressure to about 68 % bulk density does not show the theoretically predicted decline for large packing density. Probably, in the densely

packed samples particles come locally in closer contact with each other so that a coupling due to exchange interactions may become effective and complicate magnetisation structures arise which is not considered in Berkovs model.

### ACKNOWLEDGMENT

The authors thank Prof. W. Andrä for fruitful discussions and critical reading of the manuscript. They

gratefully acknowledge support with different characterisation methods: XRD by Ch. Schmidt (IPHT Jena), TEM investigations Ch. Kämnitz (University of Jena), and SEM imaging by J. Dellith (IPHT Jena). Many thanks for the laser evaporated MNP samples prepared in the group of H.-D. Kurland (University of Jena) as well as to our colleagues R. Müller and M. Zeisberger from IPHT Jena for their support.

### REFERENCES

1. W. Andrä, U. Häfeli, R. Hergt, R. Misri, *Magnetism and Advanced Magnetic Materials*, 2536 (Ed. H. Kronmüller, S. Parkin) (John Wiley & Sons Ltd: Chichester (2007).
2. Q.A. Pankhurst, N.K.T. Thanh, S.K. Jones, J. Dobson, *J. Phys. D: Appl. Phys.* **42**, 224001 (2009).
3. C.D. Mee, E.D. Daniel, *Magnetic Recording Technology* (McGraw-Hill: NewYork: 1996).
4. D.J. Dunlop, *J. Geophys. Res.* **107**, B3 (2002).
5. R. Hergt, W. Andrä, *Magnetism in Medicine*, (Ed. W. Andrä, H. Nowak) (Wiley-VCH: Berlin: 2007).
6. B. Thiessen, A. Jordan, *Int. J. Hypertherm.* **24**, 467 (2008).
7. M. Pridöhl, G. Zimmermann, A. Hartwig, A. Lühring, *Automobil-Produktion* **78** (2005)
8. R. Hergt, S. Dutz, M. Röder, *J. Phys.: Condens. Matter* **20**, 385214 (2008).
9. A.S. Eggeman, S.A. Majetich, D. Farrell, Q.A. Pankhurst, *IEEE T. Magn.* **43**, 2451 (2007).
10. D.V. Berkov, *J. Magn. Magn. Mater.* **161**, 337 (1996).
11. D.F. Eagle, J.C. Mallinson, *J. Appl. Phys.* **38**, 995 (1967).
12. A.R. Corradi, E.P. Wohlfarth, *IEEE T. Magn.* **14**, 861 (1978).
13. R.W. Chantrell, A. Bradbury, J. Popplewell, S.W. Charles, *J. Phys. D: Appl. Phys* **13**, 119 (1980).
14. R.W. Chantrell, *Magnetic Hysteresis in Novel Magnetic Materials*, (Ed. C. Hadjipanayis) (Kluwer Academic Publishers: Dordrecht: 1997).
15. L.L. Castro, M.F. da Silva, A.F. Bakuzis, R. Miotto, *J. Magn. Magn. Mater.* **293**, 553 (2005).
16. M. Klokkenburg, C. Vonk, E.M. Claesson, J.D. Meeldijk, B.H. Erné, A.P.D. Philipse, *J. Am. Chem. Soc.* **126**, 16706 (2004).
17. R.E. Dunin-Borkowski, M.R. McCartney, M. Posfai, R.B. Frankel, D.A. Bazylinski, P.R. Buseck, *Eur. J. Mineral.* **13**, 671 (2001).
18. S. Dutz, W. Andrä, R. Hergt, R. Müller, Ch. Oestreich, Ch. Schmidt, J. Töpfer, M. Zeisberger, M.E. Bellemann, *J. Magn. Magn. Mater.* **311**, 51 (2007).
19. O. Henkel, *phys. status solidi b* **7**, 919 (1964).
20. S. Dutz, M. Kettering, I. Hilger, R. Müller, M. Zeisberger, *Nanotechnology* **22**, 265102 (2011).
21. E.C.Stoner, E.P. Wohlfarth, *Phil. Trans. Roy. Soc. A* **240**, 599 (1948).
22. S. Dutz, R. Hergt, J. Mürbe, R. Müller, M. Zeisberger, W. Andrä, J. Töpfer, M.E. Bellemann, *J. Magn. Magn. Mater.* **308**, 305 (2007).
23. E. Kneller, *Physik, Band XVIII/2, Ferromagnetismus* (Ed. H.P.J. Wijn) (Springer-Verlag: Berlin-Heidelberg-New York: 1966).
24. A. Witt, K. Fabian, U. Bleil, *Earth Planet. Sc. Lett.* **233**, 311 (2005).
25. S. Dutz, R. Hergt, J. Mürbe, J. Töpfer, R. Müller, M. Zeisberger, W. Andrä, M.E. Bellemann, *Z. Phys. Chem.* **220**, 145 (2006).
26. S. Dutz, J. Clement, D. Eberbeck, T. Gelbrich, R. Hergt, R. Müller, J. Wotschadlo, M. Zeisberger, *J. Magn. Magn. Mater.* **321**, 1501 (2009).
27. R. Hergt, S. Dutz, R. Müller, M. Zeisberger, *J. Phys.: Condens. Matter* **18**, 2919 (2006).
28. H-D. Kurland, J. Grabow, G. Staupendahl, W. Andrä, S. Dutz, M.E. Bellemann, *J. Magn. Magn. Mater.* **311**, 73 (2007).
29. S. Dutz, *Nanopartikel in der Medizin*, (Verlag Dr. Kovač: Hamburg: 2008).